Water Repellent Effect and Dimension Stability of Beech Wood Impregnated with Nano-Zinc Oxide

Mojtaba Soltani,[a,]* Abdollah Najafi,[a] Samane Yousefian,[a] Hamid Reza Naji,[b] and Edi Suhaimi Bakar [b]

The objective of this study was to quantify the influence of zinc oxide nanoparticles (nano-ZnO) on the water repellency and dimensional stability of beech wood. Beech wood blocks were treated with a nano-ZnO solution at four treatment levels (0, 10,000, 20,000, and 40,000 ppm) using a modified dip method. Also, a thermal treatment was performed at 60 and 120 °C. After conditioning the samples, water absorption, volumetric swelling, water repellency effectiveness, and anti-shrink/anti-swell efficiency were determined within 24 h of soaking time. The results indicated that the nano-ZnO used for wood modification greatly improved dimensional stability and reduced the hygroscopicity of the wood. In addition, the Fourier-transform infrared spectroscopy (FTIR) analysis suggested a strong interaction between the nano-ZnO and the chemical components of wood. The heat treatment effectively improved the effects of nano-ZnO.

Keywords: Nano-zinc oxide; Beech wood; Water repellency effectiveness; Anti-swell efficiency; FTIR

*Contact information: a: Department of Wood and Paper Science and Technology, Islamic Azad University, Chalous Branch, P. O. Box 46615/397, Mazandaran, Iran; b: Faculty of Forestry, Universiti Putra Malaysia, 43400, Serdang, Selangor, Malaysia; * Corresponding author: soltani_iau@yahoo.com*

INTRODUCTION

Some characteristics of wood, such as its poor dimensional stability, durability, and flammability resistance, limit its utilization as a construction material (Fengel and Wegener 1989). Most of these drawbacks can be attributed to the hygroscopic characteristics of wood. In recent years, many methods have been used to improve wood and wood-based materials for various applications. Inorganic modification of wood and other lignocellulosic materials is one of the most widely used methods for improvement of wood properties (Mahltig *et al.* 2008; Mai and Militz 2004).

Positive attributes of these modified materials, including broadband UV absorbability, bio-degradability resistance, eco-friendly properties, and high temperature resistance, provide an opportunity for wood and lignocellulosic materials to improve their performance and function (Wegner *et al.* 2005). By incorporating inorganic components into the wood matrix, wood can be functionalized with enhanced properties in terms of water repellency and biodegradation resistance (Wang *et al.* 2012). On the other hand, nano-metal particles are available having sizes smaller than the wood pore diameters. This has led to better penetration and stabilization (Freeman and McIntyre 2008).

As a nano-metal, nano zinc oxide (nano ZnO) has some unique properties, such as non-adherent character, microcrystalline structure, as well as bacterial, fungal, and termite inhibition properties (Bak *et al.* 2012; Clousen *et al.* 2009; Kartal *et al.* 2009), UV radiation resistance (Blanchard and Blanchet 2011), and leaching resistance (Clausen *et al.* 2010).

Recent studies have revealed the effect of nano-ZnO on the reduction of water absorption of treated samples (Traistaru *et al.* 2012; Traistaru *et al.* 2013). In accordance with these studies, the most hydrophobic surfaces were observed for a system with nano-ZnO additive.

Very little is known about wood impregnation with nano-metals such as nano-ZnO. The objective of this study was to describe the effects of different concentrations of nano-ZnO on the water repellency and dimensional stability of beech wood. Effects of temperature on the performance and effectiveness of nano-ZnO were also investigated.

EXPERIMENTAL

Materials and Methods

The study was performed on wood materials from beech trees (*Fagus orientalis*) collected from the north of Iran. After oven-drying the specimens at 103±2 °C for 20 h, they were submerged in aqueous solutions of nano-ZnO (LNP-ZC brand, Lotus Nanochemistry Pars Co., Iran, at concentrations of 10,000, 20,000, and 40,000 ppm), for 1 h without dispersant and at a vacuum of 600 mm Hg to increase penetration of the solution. The nano-ZnO had a primary particle size of 20 nm. To determine the role of temperature in the treatment process, different temperatures were applied in two steps. At first, the temperature of the reactor was increased to 60 °C for 1 h. In the second step, the specimens were wrapped with aluminum foil and placed in the reactor at 120 °C for 3 h. Finally, the samples were thoroughly washed with distilled water to remove excess chemicals and then oven-dried. Untreated wood served as a control. There were seven treatment groups, as listed in Table 1.

Table 1. Treatment Groups

Testing Groups	Nano-treatment (ppm)			Temperature (ºC)	
	10000	20000	40000	60	120
Control	-----	-----	-----	-----	-----
Group 1	×	-----	-----	×	-----
Group 2	×	-----	-----	×	×
Group 3	-----	×	-----	×	-----
Group 4	-----	×	-----	×	×
Group 5	-----	-----	×	×	-----
Group 6	-----	-----	-----	×	×

×: designated treatment was conducted on samples.

The statistical analysis of the mean differences in all treatments was conducted using the Statistical Package for Social Science (PASW® statistics processor, version 15) for Windows. The data were subjected to an analysis of variance procedure to examine variability in the various properties. The Duncan multiple range test (DMRT) was used to separate the means of the various parameters at 5% probability.

Water repellency and anti-swelling efficiency

The dimensional stability of treated wood was determined by estimation of the volumetric swelling coefficient (S), anti-shrink/anti-swell efficiency (ASE), and water repellency effectiveness (WRE) using the water-soaking method (Rowell and Ellis 1978). The dimensions and weight of the oven-dried specimens were measured with a Vernier caliper with a precision of ± 0.02 mm. The specimens were submerged in distilled water for 24 h at room temperature, and the dimensions were again measured. The volumetric swelling coefficient (S), ASE, water absorption, and WRE were determined using Equations 1 through 4, respectively,

$$S\ (\%) = 100 \text{ x } (V_2\text{-}V_1)\ /V_1 \qquad (1)$$

where S is the swelling coefficient, V_2 is the volume of the saturated sample, and V_1 is the volume of the oven-dried sample.

$$ASE\ (\%) = 100 \text{ x } (S_u\text{-}S_m)\ /S_u \qquad (2)$$

In Eq. 2, ASE is the anti-swelling efficiency, whereas S_u and S_m are the swelling coefficients of unmodified and modified wood, respectively.

$$T\ (\%) = 100 \text{ x } (W_w\text{-}W_{O.D.})/W_{O.D.} \qquad (3)$$

In Eq. 3, T is the water absorption, and W_w and $W_{O.D}$ are the weights of wet and oven-dried samples, respectively.

$$WRE\ (\%) = 100 \text{ x } (T_1\text{-}T_2)\ /T_1 \qquad (4)$$

In Eq. 4, WRE is the water repellent effectiveness, and T_1 and T_2 are the rates of the water absorption of control and test specimens, respectively.

FTIR characterization

Fourier-transform infra-red spectroscopy (FTIR) has been previously used to analyze chemical changes in wood due to weathering, decay, and chemical treatments (Moor and Owen 2001). The FTIR spectra of samples were measured directly by transmission (KBr pellet technique) using a Bruker device (Vectra 22 spectrometer) in the range of 4000 to 400 cm^{-1} at 24 scan/min.

RESULTS AND DISCUSSION

FTIR

The infra-red spectra of treated and untreated wood are presented in Fig. 1. Significant changes in the FTIR spectra were obtained after modification in the region comprised of bands assigned to the main components of wood: cellulose, hemicelluloses, and lignin.

As shown, peak No.1 at wave number 3450 cm^{-1} (Fig. 1a), the intensities decreased due to the nano-treatment and temperature. This peak has been assigned to the stretching of O-H (hydroxyl) groups. The hydroxyl stretching region is particularly useful for elucidating hydrogen-bonding patterns (Poletto *et al.* 2013).

At wave numbers between 2800 and 3000 cm^{-1} (peak No. 2), the intensities decreased due to the nano-treatment. This peak has been assigned to the asymmetrical stretching of C-H methyl and methylene groups (Ding *et al.* 2012; Pandey and Pitman 2003, Papadopoulos and Mantanis 2011). Figure (1b) indicates a decreasing trend in peaks 1 and 2 due to the treatments (the arrows from top to bottom indicates the control peak at the top toward the treated peaks at the bottom).

The magnitude of the peak decreased with increasing nano-ZnO amount and with increasing temperature. In the fingerprint region (750 to 1850 cm^{-1}), many distinct peaks were observed, and these were attributed to various functional groups from wood polysaccharides (Fig. 1). The magnitudes of prominent peaks in the fingerprint region (wave number 1735 cm^{-1}) decreased in the untreated and thermal treatment groups (peak No. 3).

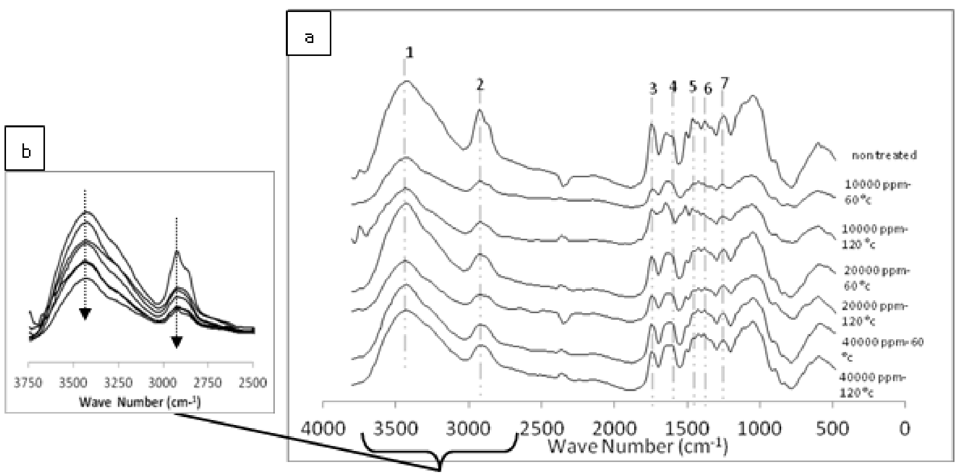

Fig. 1. FTIR spectra of non-treated and nano-ZnO-treated samples

Peak No. 3 was related to unconjugated carbonyl (C=O) stretching in xylan (Ding *et al.* 2012; Pandey and Pitman 2003). This peak indicated a partial washout of hemicellulose (Pandey *et al.* 2012). Also, at wave number 1504 cm^{-1} (peak No. 4), the intensities decreased as a result of the treatments. This peak has been assigned to an aromatic skeletal vibration in lignin (C=C stretch) (Bak *et al.* 2012; Pandey and Pitman 2003; Papadopoulos and Mantanis 2011). There was also a significant decrease in the peak at 1457 cm^{-1} (peak No. 5) with increasing treatment intensity that was seemingly related to C-H deformation in lignin (as CH_2 and CH_3, the aliphatic part of lignin) and carbohydrates (Pandey *et al.* 2012). Another peak at wave number 1373 cm^{-1} (peak No. 6), which has been assigned to C-H (CH_3 bonding), indicating deformation in cellulose and hemicellulose (Ding *et al.* 2012; Pandey and Pitman 2003), decreased due to the treatments (Fig. 1). A prominent peak (No. 7) between 1230 and 1249 cm^{-1} decreased in the treated samples compared to the control group. This peak has been assigned to C-O stretching and C=O deformation in lignin and xylan for the syringyl ring (the major type of hardwood lignin) (Ding *et al.* 2012; Pandey and Pitman 2003).

In addition to other reported characteristics, such as good penetration, effective size, and uniform distribution, from the effects of nano-ZnO (Clausen *et al.* 2010;

Clousen *et al.* 2009; Freeman and McIntyre 2008), the results suggested a strong interaction between the nano-ZnO and the chemical components of wood. FTIR spectroscopy showed that the lignin and hemicellulose components of wood were affected due to the treatments. Nano treatment and temperature clearly decreased the amounts of hydroxyl groups (at 3450 cm^{-1}) and influenced on lignin, as confirmed by the reduction in the peaks at 1249, 1457, and 1504 cm^{-1} assigned to aromatic skeletal vibrations. Also, the reduction in the peaks at 1735 and 1373 cm^{-1} indicated a partial washout of hemicellulose.

Some authors have assigned other peaks to ZnO, such as 2865-2971 cm^{-1} (Traistaru *et al.* 2012), 3419 cm^{-1} (AbdElhady 2012), and 3409 cm^{-1} (Salehi *et al.* 2010). However, these peaks are not really characteristic of ZnO, and a registration of FTIR spectra between 400 and 500 cm^{-1} could have demonstrated the presence of ZnO (Kloprogge *et al.* 2004; Traistaru *et al.* 2012).

Water Absorption – Volumetric Swelling

The average water absorption and volumetric swelling in the control and nano-ZnO-treated specimens at different temperatures are illustrated in Fig. 2. The average water absorption percentage significantly decreased with increasing nano-intensity. The nano-concentration of 40,000 ppm showed the lowest water absorption, and there was a decreasing trend as the temperature increased from 60 °C to 120 °C for each nano-intensity.

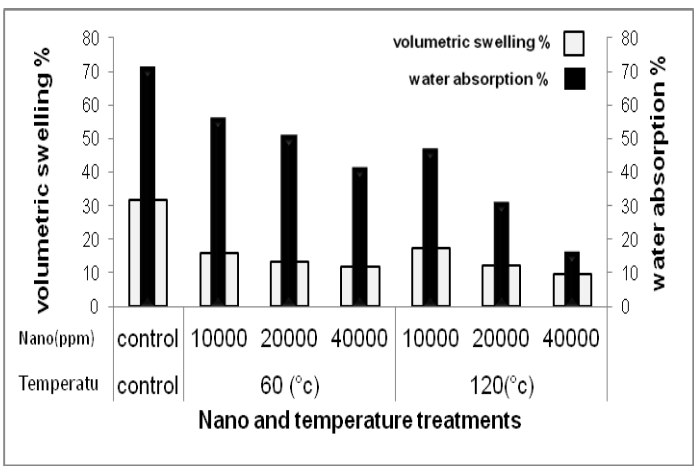

Fig. 2. Effect of nano-ZnO and temperature on volumetric swelling and water absorption

The nano treatment significantly decreased the swelling of the impregnated wood compared to the control sample (Fig. 2). However, the effect of temperature on volumetric swelling was not significant ($p < 0.05$). The lowest values were obtained at a nano-concentration of 40,000 ppm and a temperature of 120 °C. The reduction in water absorption and volumetric swelling with increasing nano-intensity suggested that higher concentrations of nano-ZnO provided substantial water resistance (Clausen *et al.* 2010).

Anti-Swelling Efficiency (ASE) – Water Repellency Effectiveness (WRE)

The variations in ASE with different nano-treatment intensities and temperatures are presented in Fig. 3. The results showed that the uppermost ASE was obtained at a concentration of 40,000 ppm and 120 °C.

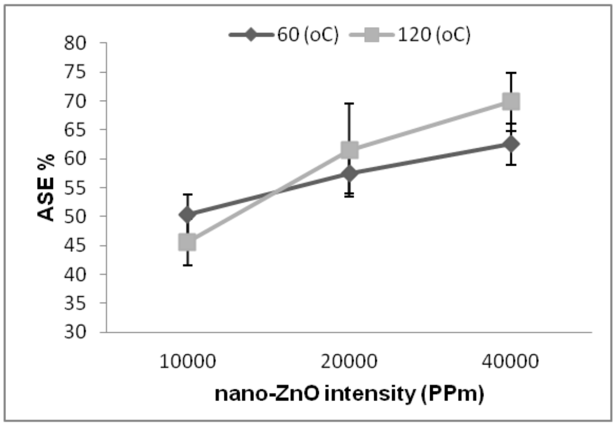

Fig. 3. Effect of nano-ZnO intensity on anti-swelling efficiency

Variation in the WRE of the samples soaked for 24 h in water was observed as a result of the different nano-ZnO intensity and temperature treatments (Fig. 4). The moisture behavior of beech wood was significantly affected by the nano-ZnO and temperature treatments in the impregnating process. The results showed that the nano and thermal treatment intensities increased the WRE percentage. However, a temperature of 120 °C had a more prominent effect on WRE than did a temperature of 60 °C.

A temperature treatment of 60 °C achieved a minimum WRE (20%) at a nano-intensity of 10,000 ppm, while about 77% WRE was achieved at a temperature of 120 °C with a nano-intensity of 40,000 ppm.

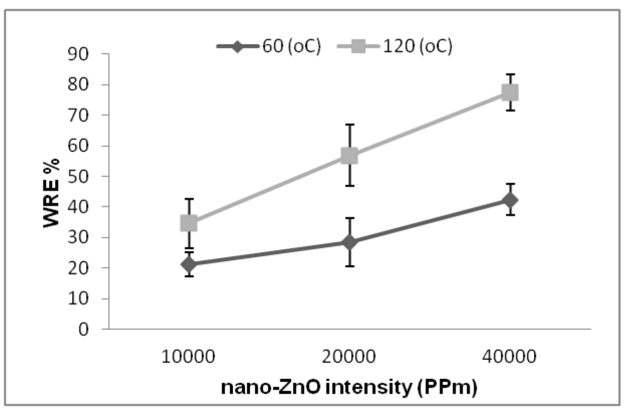

Fig. 4. Effect of nano-ZnO intensity on water repellency effectiveness

The moisture behavior of wood is controlled by a complex mechanism (Rautkari *et al.* 2013). Based on the literature, the good penetration, effective size, and uniform distribution of nano-ZnO may reduce the hygroscopicity and improve the dimensional stability (Clausen *et al.* 2009, 2010; Freeman and McIntyre 2008). On the other hand, It has to be noted that the increasing of ASE and WRE may result in reducing the hydroxyl group contents and accessibility in treated samples (Hill *et al.* 2010; Rowell 1980). Moreover, the hemicelluloses are the most labile and hydrophilic wood polymer. Hence, reduced hygroscopicity could resulted in degradation and washout of hemicelluloses due to the nano-ZnO treatment (Rautkari *et al.* 2013).

CONCLUSIONS

1. Based on the current study, a reduction in the hygroscopicity of the wood could be attributed to the nano-treatment with ZnO. The anti-swelling efficiency (ASE) was found to depend upon the extent of the treatments, and its value increased with increasing nano-intensity and temperature.
2. The dimensional stability of the wood was greatly improved by modification with the nano-ZnO. In addition, the nano-ZnO had strong interaction with the chemical constituents of wood. These responses were proven by FTIR spectroscopy and can be used to explain the moisture behavior of the chemical components of wood such as hemicellulose and lignin.
3. The temperature of the process was the most influential parameter for improving the functionality of the ZnO-nano particles. It therefore appears that nano-ZnO treatment can be a useful option to reduce the hygroscopicity and improve the dimensional stability of wood.

REFERENCES CITED

AbdElhady, M. M. (2012). "Preparation and characterization of chitosan/zinc oxide nanoparticles for imparting antimicrobial and UV protection to cotton fabric," *International Journal of Carbohydrate Chemistry*, 1-6.

Bak, M., Yimmou, B. M., Csupor, K., Németh, R., and Csóka, L. (2012). "Enhancing the durability of wood against wood destroying fungi using nano-zinc," *International Scientific Conference on Sustainable Development & Ecological Footprint*

Blanchard, V., and Blanchet, P. (2011). "Color Stability for wood products during use: effects of inorganic nanoparticles," *BioResources* 6, 1219-1229.

Clausen, C. A., Green, F., and Kartal, S. N. (2010). "Weatherability and leach resistance of wood impregnated with nano-zinc oxide," *Nanoscale Research Letters* 1464-67.

Clousen, C. A., Yang, V. W., Arang, R. A., and Green, F. (2009). "Feasibility of nanozinc oxide as a wood preservative," *American Wood Protection Association - Proceeding* 105, 255-260.

Ding, W. D., Kaubaa, A., and Chaala, A. (2012). "Dimensional Stability of methyl methacrylate hardened hybrid poplar wood," *BioResources* 7, 504-520.

Fengel, D., and Wegener, G. (1989). *Wood: Chemistry, Ultrastructure, Reactions*, Walter de Gruyter, Berlin.

Freeman, M. H., and McIntyre, C. R. (2008). "Comprehensive review of copper-based wood preservatives," *Forest Products Journal* 58, 21-27.

Hill, C. A., Norton, A. J., and Newman, G. (2010). "The water vapour sorption properties of Sitka spruce determined using a dynamic vapour sorption apparatus," *Wood Science and Technology* 44, 497-514.

Kartal, S. N., Green, F., and Clausen, C. A. (2009). "Do the unique properties of nanometals affect leachability or efficacy against fungi and termites?" *International Biodeterioration & Biodegradation* 63, 490-495.

Kloprogge, J. T., Hickey, L., and Frost, R. L. (2004). "FT-Raman and FT-IR spectroscopic study of synthetic Mg/Zn/Al-hydrotalcites," *Journal of Raman Spectroscopy* 35, 967-974.

Mahltig, B., Swaboda, C., Roessler, A., and Böttcher, H. (2008). "Functionalising wood by nanosol application," *Journal of Materials Chemistry* 18, 3180-3192.

Mai, C., and Militz, H. (2004). "Modification of wood with silicon compounds. inorganic silicon compounds and sol-gel systems: A review," *Wood Science and Technology* 37, 339-348.

Moor, A. K., and Owen, N. L. (2001). "Infrared spectroscopic studies of solid wood," *Applied Spectroscopy Reviews* 36, 65-86.

Pandey, J. K., Lee, S., Kim, H., Tankagi, H., Lee, C. S., and Ahn, S. H. (2012). "Preparation and properties of cellulose-based nano composites of clay and polypropylene," *Journal of Applied Polymer Science* 125, 651-660.

Pandey, K. K., and Pitman, A. J. (200)3. "FTIR studies of the changes in wood chemistry following decay by brown-rot and white-rot fungi," *International Biodeterioration & Biodegradation* 52, 151-60

Papadopoulos, A. N., and Mantanis, G. I. (2011). "Surface treatment technologies applied to wood surfaces," *FDM Asia-Solid Wood and Panel Technology* May/June, 36-39.

Poletto, M., Pistor, V., and Zattera, A. J. (2013). *Structural Characteristics and Thermal Properties of Native Cellulose*. In: Cellulose-fundamental aspects. Ed. Van de Ven, T. and Gdbout, L. *InTech.* 45-68.

Rautkari, L., Hill, C. A. S., Curling, S., Jalaludin, Z., and Ormondroyd, G. (2013). "What is the role of the accessibility of wood hydroxyl groups in controlling moisture content ?" *Journal of Material Science* 48, 6352-6356.

Rowell, R. M. (1980). "Distribution of reacted chemicals in southern pine modified with methyl isocyanate," *Wood Science* 13, 102-110.

Rowell, R. M., and Ellis, W. D. (1978). "Determination of dimensional stabilisation of wood using the watersoak method," *Wood and Fiber Science* 10, 104-111.

Salehi, R., Arami, M., Mahmoodi, N. M., Bahrami, H., and Khorramfar, S. (2010). "Novel biocompatible composite (Chitosan-zinc oxide nanoparticle): Preparation, characterization and dye adsorption properties," *Colloids and surfaces. B, Biointerfaces* 80, 86-93.

Traistaru, A.-aT., Timar, M. C., Campean, M., Croitoru, C., and Sandu, I. O. N. (2012). "Paraloid B72 versus Paraloid B72 with nano-ZnO additive as consolidants for wooden artefacts," *Materiale Plastice* 49, 293-300.

Traistaru, A.-aT., Timar, M. C., Campean, M., Croitoru, C., and Sandu, I. O. N. (2013). "SEM-EDX, water absorption, and wetting capability studies on evaluation of the influence of nano-zinc oxide as additive to paraloid B72 solutions used for wooden artifacts consolidation," *Microscopy Research and Technique* 76, 209-218.

Wang, X., Liu, J., and Chai, Y. (2012). "Thermal, mechanical, and moisture absorption properties of wood-TiO_2 composites properties prepared by a sol-gel process," *BioResources* 7(1), 893-901.

Wegner, T., Winandy, J., and Ritter, M. (2005). "Nanotechnology opportunities in residential and nonresidential construction," 2nd International Symposium on Nanotechnology in Construction, Bilbao, Spain., 8.

Article submitted: August 19, 2013; Peer review completed: September 11, 2013; Revised version received and accepted: October 16, 2013; Published: October 22, 2013.